Effect of Parallel Radiofrequency Transmission on Arterial Input Function Selection in Dynamic Contrast-Enhanced 3 Tesla Pelvic MRI

Hatim Chafi, BS,[1,2] Saba N. Elias, MS,[3] Huyen T. Nguyen, PhD,[3] Harry T. Friel, MS,[4] Michael V. Knopp, MD, PhD,[3] BeiBei Guo, PhD,[5] Steven B. Heymsfield, MD,[2] and Guang Jia, PhD[1,2]*

Background: To evaluate whether parallel radiofrequency transmission (mTX) can improve the symmetry of the left and right femoral arteries in dynamic contrast enhanced magnetic resonance imaging (DCE-MRI) of prostate and bladder cancer.

Methods: Eighteen prostate and 24 bladder cancer patients underwent 3.0 Tesla DCE-MRI scan with a single transmission channel coil. Subsequently, 21 prostate and 21 bladder cancer patients were scanned using the dual channel mTX upgrade. The precontrast signal (S_0) and the maximum enhancement ratio (MER) were measured in both the left and the right femoral arteries. Within the patient cohort, the ratio of S_0 and MER in the left artery to that in the right artery (S_0_LR, MER_LR) was calculated with and without the use of mTX. Left to right asymmetry indices for S_0 ($S_0\_LR_{asym}$) and MER (MER_LR_{asym}) were defined as the absolute values of the difference between S_0_LR and 1, and the difference between MER_LR and 1, respectively.

Results: $S_0\_LR_{asym}$, and MER_LR_{asym} were 0.21 and 0.19 for prostate cancer patients with mTX, and 0.43 and 0.45 for the ones imaged without it ($P < 0.001$). Also, for the bladder cancer patients, $S_0\_LR_{asym}$, and MER_LR_{asym} were 0.11 and 0.9 with mTX, while imaging without it yielded 0.52 and 0.39 ($P < 0.001$).

Conclusion: mTX can significantly improve left-to-right symmetry of femoral artery precontrast signal and contrast enhancement.

J. MAGN. RESON. IMAGING 2015;00:000–000.

The use of high magnetic field strength for MRI ($\geq$ 3.0 Tesla [T]) suffers from radiofrequency (RF) excitation field inhomogeneity.[1] Left-to-right signal symmetry on axial/coronal pelvic MR images is negatively affected by B1 field inhomogeneity.[2] The dielectric artifact is a nonuniform RF distribution caused by variations of the RF wave, variations that result from the formation of standing waves in tissue.[2] Scanners with single channel RF transmission may produce images with spatially-varying image contrast and signal intensity due to this dielectric artifact.[3] Parallel RF transmission (mTX), by contrast, minimizes the dielectric artifact through the use of multiple channels.[2] This results in an image with uniform signal and contrast. In addition, image quality, such as signal-to-noise ratio (SNR), has been shown to be improved with mTX in diffusion weighted imaging (DWI).[4] mTX can also increase image contrast in cardiac MRI and reduce the off-resonance artifact.[5]

Prostate cancer will account for 26% (220,800) of incident cases in United States of America men in 2015.[6] Multiparametric MRI, which refers to T2-weighted anatomical images and other functional imaging methods (such as dynamic contrast-enhanced MRI (DCE-MRI), DWI, and MR spectroscopic imaging) is regarded as the best available tool for the clinical imaging of prostate cancer.[7] Multi-parametric

View this article online at wileyonlinelibrary.com. DOI: 10.1002/jmri.24969

Received Sep 16, 2014, Accepted for publication May 22, 2015.

*Address reprint requests to: Guang Jia, Department of Physics and Astronomy, Baton Rouge, LA, 70803. E-mail: gjia@lsu.edu

From the [1]Department of Physics and Astronomy, Louisiana State University, Baton Rouge, Louisiana, USA; [2]Pennington Biomedical Research Center, Baton Rouge, Louisiana, USA; [3]Department of Radiology, The Ohio State University, Columbus, Ohio, USA; [4]Philips Healthcare, Highland Heights, Ohio, USA; and [5]Department of Experimental Statistics, Baton Rouge, Louisiana, USA

MRI significantly increases the area under the receiver operating characteristic curve for cancer detection in the peripheral zone (PZ) in comparison to T2-weighted images alone.[8]

DCE-MRI measures the variation in T1-weighted signal intensity over time before and after the injection of a contrast agent. The Gd-based contrast agent exchanges between the intravascular space and the extravascular extracellular space (EES) at a rate dependent on tissue environment and microcirculation.[9] The T1 values of blood and interstitial water are altered by the contrast agent concentration. The time concentration curve of the contrast agent can be calculated by normalizing the signal intensity to what it would be without the presence of the contrast agent.[10] In addition, compartmental analysis can be used to obtain tissue parameters, such as the volume transfer constant between blood plasma and EES (K^{trans}), the rate constant between EES and blood plasma (k_{ep}), and the volume of EES per unit volume of tissue (v_e).[11] k_{ep}, K^{trans}, and v_e were found to be significantly higher in tumor than in normal PZ Tissue.[12–14]

Bladder cancer will account for 4.4% of all United States cancer cases in 2015.[6] DCE-MRI of the bladder has shown good interobserver agreement and high accuracy in the differentiation of superficial versus invasive disease and organ-confined versus non–organ-confined tumors.[15] Compared with T2 weighted MRI, The supplementation of DCE-MRI improved interobserver agreement as well as the localization of small malignant tumors and those within bladder wall thickening.[16]

Determining pharmacokinetic parameters demands the knowledge of contrast agent concentration in the feeding artery as a function of time; this is commonly referred to as the arterial input function (AIF).[17] In pelvic DCE-MRI, it is convenient to measure the AIF in the femoral arteries. An underlying issue that often arises in this situation, however, is which of the two femoral arteries to measure. The inhomogeneity produced by single RF transmission scanners could result in left-to-right asymmetry of the femoral arteries. This would affect AIF selection, and an over estimation of the AIF would result in an underestimation of K^{trans} and v_e.[11]

The aim of this study is to evaluate whether parallel RF transmission can improve the symmetry of the left and right femoral artery signal intensity in DCE-MRI of prostate and bladder cancer.

Materials and Methods

Phantom

A phantom was built using twelve 8-mL tubes with a diameter (1.3 cm) comparable to that of the femoral arteries. Gd-based contrast agent (Magnevist; Bayer Health Care) was dissolved in distilled water. Two groups of six tubes were placed contralateral to each other on top of a 3 Tesla (T) compatible cylindrical phantom filled with mineral oil (Fig. 1). In each group, the Gd-based contrast agent concentrations selected were 0, 0.05, 0.1, 0.15, 0.25, and 0.4 mM.

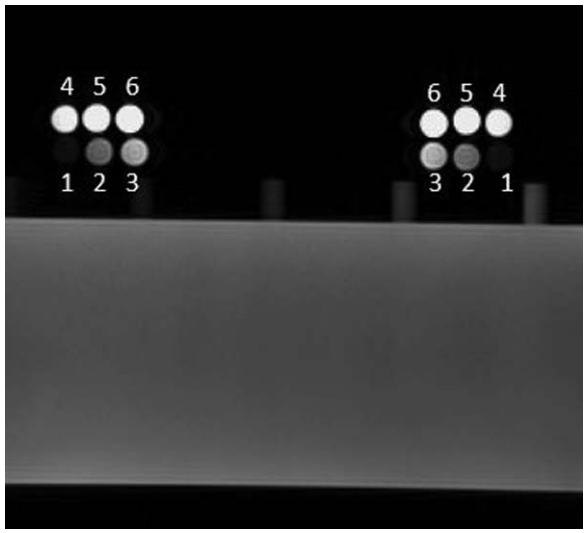

FIGURE 1: Two groups of tubes of varying concentrations were placed on top of a 3T compatible phantom filled with mineral oil. Concentrations of Gd-based contrast agent were arranged in each group as 1 (0.00 mM), 2 (0.05 mM), 3 (0.10 mM), 4 (0.15 mM), 5 (0.25 m), and 6 (0.40 mM).

Subjects

The retrospective patient study was approved by the local institutional review board. From April 2008 to August 2013, a total of 39 prostate (age range, 43–79 years; median, 62 years) and 45 bladder cancer (age range, 38–83 years; median, 67 years) patients were enrolled in this study. All cases were confirmed by biopsy and referred for MRI by urologists.

Imaging

From April 2008 to June 2010, 18 prostate and 24 bladder cancer patients were scanned on a 3.0T MRI system (Achieva; Philips Healthcare, Netherland, Best) using a single channel RF transmit Q-body and 32-channel phased-array surface coils. From August 2010 to June 2013, 21 prostate and 21 bladder cancer patients were scanned on the same 3.0T MRI system using a two-channel RF transmit upgrade and 32-channel phased-array surface coils.

DCE-MRI sequence parameters for phantom, prostate, and bladder protocols are shown in Table 1. Both Protocols had a single dose (0.2 mmol per kilogram body weight) of Gd-based contrast agent (Magnevist; Bayer Health Care, or Multihance; Bracco) intravenously injected at a constant flow rate of 0.5 mL/s after the fifth phase, followed by a flush of 25 mL of saline at a flow rate of 2 mL/s. The phantom was imaged using the DCE-MRI prostate protocol (number of slices, 30; number of dynamic scans, 6) with mTX, and once again with the mTX turned off.

Phantom Image Analysis

For a single spatial slice, an ROI was drawn on each tube and the average signal intensity over all 6 temporal phases was measured. The ratio of average signal intensity (S) to the average signal intensity for distilled water (S_0) was subtracted by one. This quantity was plotted as a function of the concentration, and fitted linearly for the right and left group of tubes for the phantom imaged with and without mTX. A linear fit was chosen because for a two-compartment pharmacokinetic model, the theoretical signal

TABLE 1. Parameters for Prostate and Bladder DCE-MRI Protocol

	Phantom protocol	Prostate protocol		Bladder protocol
	Without mTX and with mTX	Without mTX	With mTX	Without mTX and with mTX
Sequence type	3D SPGE	3D SPGE	3D SPGE	3D SPGE
Coil	Q-Body, 32-channel	Q-Body, 32-channel	Q-Body, 32-channel	Q-body, 32-channel
TR (ms)	5	7.6	5	5
TE (ms)	1.51	1.6–3.9	1.51	2
Slice thickness (mm)	6	6	6	5
Flip angle (°)	20	20	20	20
Matrix	192 × 192	192 × 192	192 × 192	214 × 214
Field of view (mm)	220	150–172	150–172	95
NEX	1	1	1	1
Temporal resolution (s)	8.8	5.4–14.1	8.8	8.3
Number of dynamic scans	6	30–59	40	60

3D SPGE, 3 dimensional spoiled gradient echo; TE, echo time; TR, repetition time; NEX, number of signal averages.

enhancement from Gd-DTPA enhanced dynamic 3D gradient-recalled images has a linear relationship with tissue concentration.[18] The signal enhancement is related to concentration as:

$$\frac{S}{S_0} = 1 = k[Gd] \quad (1)$$

where k is T_{10} r_1 and $[Gd]$ is the concentration of the contrast agent. T_{10} is the T_1 before the injection of the Gd-DTPA, and r_1 is its relaxivity. k was determined from the linear fit, and the ratio of k for the left group of tubes to k for the right group of tubes (k_LR) was calculated for the phantom imaged with and without mTX.

Subject Image Analysis

DCE-MRI data was processed in an IDL (Exelis Visual Information Solutions, Boulder, CO) based software environment by manually drawing a region of interest (ROI) in the right and left femoral arteries of each patient for a single spatial slice. The slice was selected on the basis that it would be sufficiently distal within the axial 3D slab to avoid saturation from in-flow blood, and slice-selection gradient imperfection on border slices.[19]

The time signal intensity curve of the femoral artery is seen in Figure 2; the precontrast signal S_0 was defined as the average of baseline signals in the femoral artery. Maximum enhancement ratio (MER) was defined by:

$$MER = \frac{S_{max} - S_0}{S_0} \quad (2)$$

where S_{max} is the maximum signal intensity with contrast enhancement in the femoral artery. For each single slice, time signal intensity curves were measured in both femoral ROIs. All time signal intensity curves were acquired by a single observer. Asymmetry for S_0 ($S_0\_LR_{asym}$) was defined by:

$$S_0\_LR_{asym} = |S_0\_LR - 1| \quad (3)$$

where the S_0_LR is the ratio of S_0 in the left artery ROI to S_0 in the right artery ROI. Asymmetry for MER (MER_LR_{asym}) was defined by:

$$MER\_LR_{asym} = |MER\_LR - 1| \quad (4)$$

where the MER_LR is the ratio of MER in the left artery ROI to the MER in the right artery ROI. A left-to-right symmetry of 1 and a left-to-right asymmetry of 0 would indicate an ideal symmetrical case.

Statistical Analysis

S_0_LR, MER_LR, $S_0\_LR_{asym}$, and MER_LR_{asym} were compared between the patients imaged with and without mTX by using a student t-test. A P-value of <0.05 was considered to indicate a significant difference. The statistical analysis was performed using Microsoft Excel 2010 (Microsoft Corporation, Redmond, WA).

Results

The mean ratio of S_0_LR was 1.41 ± 0.42 for the prostate cancer patients imaged on the 3T scanner without mTX, and 1.17 ± 0.20 for the prostate cancer patients imaged on the 3T scanner with mTX (P=0.037). The mean $S_0\_LR_{asym}$ was 0.43 ± 0.39 for prostate cancer patients imaged on the 3T scanner without mTX and 0.21 ± 0.16 for prostate cancer patients imaged on the 3T scanner with mTX ($P < 0.001$).

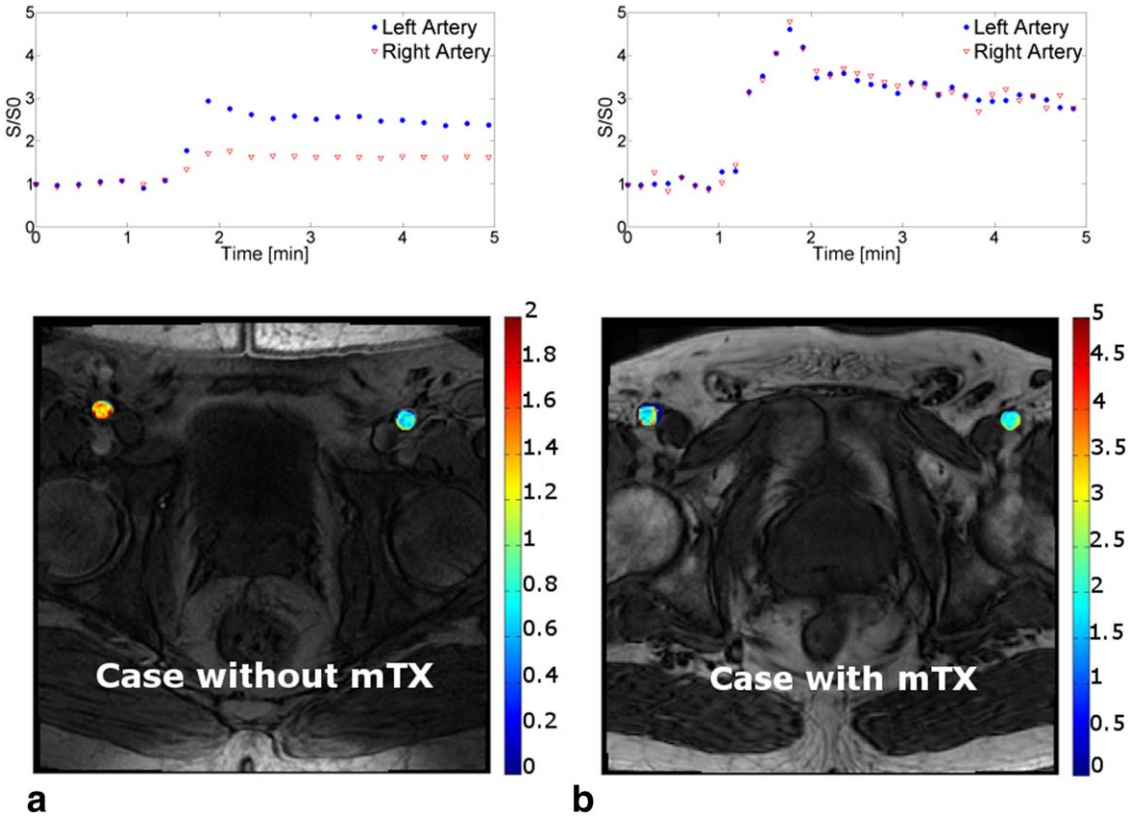

FIGURE 2: The signal enhancement as a function of time and MER map in the femoral arteries overlaid on a T1 weighted image obtained with a single RF transmission channel (A). The signal enhancement as a function of time and MER map overlaid on a T1 weighted image obtained with a dual RF transmission channel (B).

Figure 3A contains a boxplot depicting the full range variation of $S_0\_LR_{asym}$ with and without mTX.

The average ratio of *MER_LR* was 0.55 ± 0.15 for patients imaged on the 3T scanner without mTX, and 0.91 ± 0.21 for prostate cancer patients imaged on the 3T scanner with mTX ($P = 0.031$). The mean MER_LR_{asym} was 0.45 ± 0.15 for prostate cancer patients imaged without the mTX upgrade, and 0.19 ± 0.14 for prostate cancer patients imaged with the mTX upgrade ($P < 0.001$) (Fig. 3B).

The mean ratio of S_0_LR was 1.42 ± 0.48 for the bladder cancer patients imaged on the 3T scanner without mTX, and 1.03 ± 0.17 for the bladder cancer patients imaged on the 3T scanner with mTX ($P < 0.001$). The mean $S_0\_LR_{asym}$ was 0.52 ± 0.37 for bladder cancer patients imaged on the 3T scanner without mTX and 0.11 ± 0.13 for bladder cancer patients imaged on the 3T scanner with mTX ($P < 0.001$) (Fig. 3A).

The average ratio of *MER_LR* was 0.80 ± 0.38 for bladder cancer patients imaged on the 3T scanner without mTX, and 1.01 ± 0.11 for bladder cancer patients imaged on the 3T scanner with mTX ($P = 0.014$). The mean MER_LR_{asym} was 0.37 ± 0.20 for bladder cancer patients imaged without the mTX upgrade, and 0.09 ± 0.07 for bladder cancer patients imaged with the mTX upgrade ($P < 0.001$) (Fig. 3B).

Figure 4 shows a plot of the $\frac{S}{S_0} - 1$ as a function of concentration for the right and left groups of tubes for the phantom imaged with and without mTX. *k_LR* was 0.88 ± 0.04 for the phantom imaged without mTX, and 0.93 ± 0.05 when imaged with mTX.

Discussion

The goal of this work was to assess whether parallel RF transmission can improve the symmetry of the left and right femoral artery signal intensity in pelvic DCE-MRI. Parallel RF transmission has shown a reduction in asymmetry of baseline and signal enhancement. Phantom data also indicated improvement in symmetry between vials of the same concentration placed contralaterally. This makes a strong case for the variation of the parameters used for the prostate cancer patient having no effects on the asymmetry. Previous work has been done to assess the effect of parallel RF transmission on pelvic imaging.[2] However, this assessment is of its impact on T1 and T2-weighted image quality. Our work focuses on the effect of parallel RF transmission on quantitative imaging, specifically its effect on AIF selection in DCE-MRI. We also evaluated this effect by imaging prostate and bladder cancer patients as oppose to volunteers.[2] S_0 and MER measured in the femoral artery are commonly used parameters in quantitative pelvic DCE-MRI analysis. A

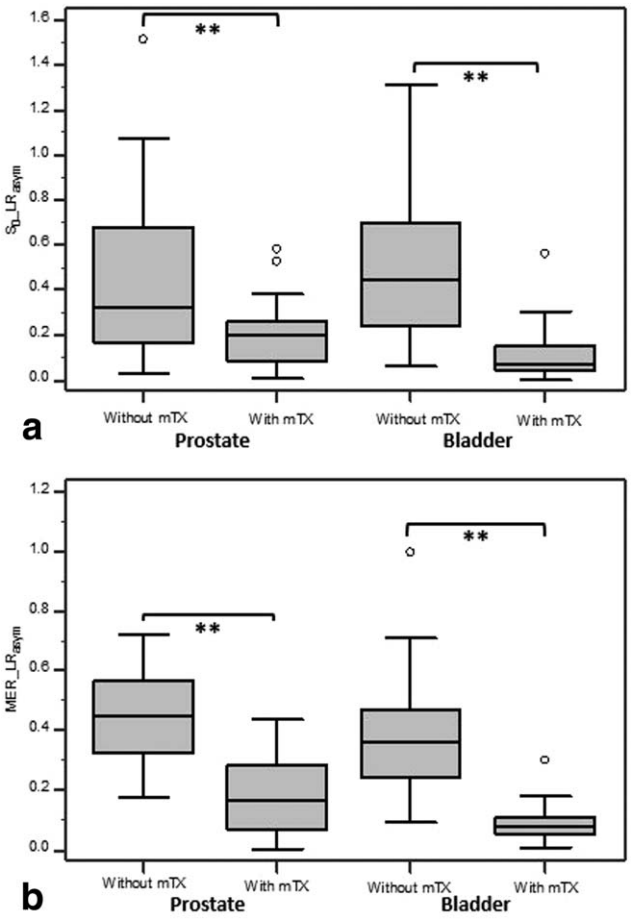

FIGURE 3: Boxplots displaying the full range of variation (from minimum to maximum) of S_0_LR_{asym} (A) and MER_LR_{asym} (B) for prostate and bladder patients imaged with and without mTX . **$P < 0.001$.

symmetrical S_0 and MER in both femoral arteries could improve the reproducibility of manual AIF measurements. Also, the process required to compare both ROIs in the left and right femoral arteries, would be eliminated if AIF measurements were more likely to be symmetrical.

Increasing the number of transmit channels has been shown to increase the RF homogeneity, and decrease specific absorption in the pelvis.[2] Using a five point scale adapted from Willinek et al.[20] a blind grading system was used to assess variation in imaging performance. Axial T1-weighted images were found to increase in perceived image performance with channel numbers for pelvic imaging. Our results showed that the symmetry between the precontrast signal, and enhanced signal in the femoral arteries, improved significantly in T1-weighted images acquired with mTX. Symmetry is an indirect measure of homogeneity.

The effect of parallel RF transmission 3.0T cardiac MR imaging has been studied.[5] Subjects were scanned with single and dual source transmission. It was shown that RF transmission with patient-adaptive RF shimming can significantly improve RF field inhomogeneity and increase contrast of cardiac balanced-turbo field echo cine images. A reduction in off-resonance image artifacts was also observed. The prostate is smaller than the heart; however, it is also adjacent to an air-filled organ. Cardiac wall imaging is similar to imaging the bladder wall. Off-resonance artifacts could result in geometric distortion in the bladder wall which could lower the accuracy of bladder cancer diagnosis. Parallel RF transmission was shown to achieve consistent good diagnostic image quality on T2-weighted images.[16] A comparison in diagnostic performance between 1.5T endorectal coil MRI and 3.0T nonendorectal coil MRI was conducted in prostate cancer.[21] Nonendorectal coil 3.0T MRI enables prostate image acquisition of comparable image quality to those obtained with 1.5T endorectal coil MRI. A similar study design should be implemented in future studies to investigate whether parallel RF transmission can improve prostate cancer detection.

DWI was performed with single source and dual source transmission.[4] In the abdomen, measured apparent diffusion coefficient of lateral left hepatic lobe and spleen at b-value combinations of 0/100 and 0/800 s/mm^2 were significantly different between dual-source and single-source images. DWI is used in conjunction with DCE MRI in Multi-parametric prostate cancer MRI.[22] It is also used to image lymph nodes metastases from prostate cancer.[23] Future work should be conducted to evaluate the effect of DWI combined with parallel RF transmission on region-based lymph node analysis in high-risk prostate cancer patients.

This study had the following limitations. Patients were not scanned using both dual source RF transmission and single source RF transmission. There could have been inter-

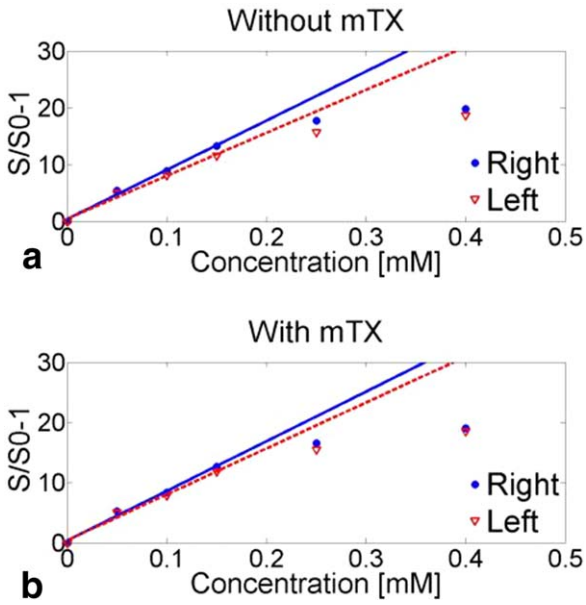

FIGURE 4: Plot of the $\frac{S}{S_0} - 1$ as a function of contrast agent concentration for the phantom imaged without mTX. The right and left groups of vials were fitted linearly (A). Plot of the $\frac{S}{S_0} - 1$ as function of contrast agent concentration for the phantom imaged with mTX. The right and left groups of vials were fitted linearly (B).

subject variations that might have affected the results. Our work did not evaluate the effect of parallel RF transmission on DCE-MRI related motion artifacts due to under sampling which is needed to achieve high temporal resolution, or motion related artifacts resulting from respiration. We attempted to simulate femoral arteries by constructing a phantom. The phantom had two groups of vials with varying contrast agent concentrations placed contralaterally. However, for simplicity and practicality, Gd-based contrast agent was dissolved in distilled water instead of blood. Blood is multicompartmental in comparison to aqueous solution, and consists of red blood cells and plasma.[24] It also contains hemoglobin which affects the susceptibility mismatch between the two compartments. For the prostate patients, several parameters varied due to efforts at enhancing and standardizing the institutional DCE-MRI protocol. It is possible that having different acquisition parameters used for the prostate patients could have impacted symmetry. However, this is unlikely due to all of the bladder cancer patients being imaged using the same acquisition parameters with and without mTX, which yielded a comparable outcome. Sometimes multiple channel transmission may not give satisfactory radiofrequency B1 field homogeneity. Several B1 mapping techniques have been introduced. The standard double method is a long TR acquisition.[25] whereby an image is acquired at a prescribed flip angle, α, and then at twice that 2α, from which the true flip angle can be determined by using the trigonometric double angle formula. Contrast enhanced femoral artery signal intensity in DCE-MRI can be corrected based on this B1 mapping technique.

In conclusion, S_0 and MER symmetry in the femoral arteries were improved with mTX in comparison to single source transmission. The phantom results showed improved left to right symmetry of the linear relationship between signal enhancement and concentration. High field (3.0T) MRI scanner equipped with multiple-channel parallel RF transmission ameliorated the symmetry of AIF in femoral arteries. This technology could result in more consistent and homogeneous quantitative pharmacokinetic modeling in prostate and bladder cancer DCE-MRI.

Acknowledgments

Contract grant sponsor: National Institutes of Health; Contract grant number: R21CA156945; Contract grant sponsor: the American Urological Association Foundation Research Scholars Program; Contract grant sponsor: EUSA Pharma (USA), Inc.

References

1. van den Bergen B, Stolk CC, Berg JB, Lagendijk JJ, Van den Berg CA. Ultra fast electromagnetic field computations for RF multi-transmit techniques in high field MRI. Phys Med Biol 2009;54:1253–1264.
2. Childs AS, Malik SJ, O'Regan DP, Hajnal JV. Impact of number of channels on RF shimming at 3T. MAGMA 2013;26:401–410.
3. Jiang L, Zhou Y, Zhou C, et al. Dual-source parallel radiofrequency transmission for magnetic resonance breast imaging at 3T: any added clinical value? Magn Reson Imaging 2014;32:523–528.
4. Guo L, Liu C, Chen W, Chan Q, Wang G. Dual-source parallel RF transmission for diffusion-weighted imaging of the abdomen using different b values: image quality and apparent diffusion coefficient comparison with conventional single-source transmission. J Magn Reson Imaging 2013;37:875–885.
5. Jia H, Wang C, Wang G, et al. Impact of 3.0 T cardiac MR imaging using dual-source parallel radiofrequency transmission with patient-adaptive B1 shimming. PloS One 2013;8:e66946.
6. Siegel RL, Miller KD, Jemal A. Cancer statistics, 2015. CA Cancer J Clin 2015;65:5–29.
7. Nguyen PL, Aizer A, Assimos DG, et al. ACR Appropriateness criteria (R) definitive external-beam irradiation in stage T1 and T2 prostate cancer. Am J Clin Oncol 2014;37:278–288.
8. Delongchamps NB, Rouanne M, Flam T, et al. Multiparametric magnetic resonance imaging for the detection and localization of prostate cancer: combination of T2-weighted, dynamic contrast-enhanced and diffusion-weighted imaging. BJU Int 2011;107:1411–1418.
9. Shukla-Dave A, Hricak H. Role of MRI in prostate cancer detection. NMR Biomed 2014;27:16–24.
10. Verma S, Turkbey B, Muradyan N, et al. Overview of dynamic contrast-enhanced MRI in prostate cancer diagnosis and management. AJR Am J Roentgenol 2012;198:1277–1288.
11. Tofts PS, Brix G, Buckley DL, et al. Estimating kinetic parameters from dynamic contrast-enhanced T(1)-weighted MRI of a diffusable tracer: standardized quantities and symbols. J Magn Reson Imaging 1999;10:223–232.
12. Buckley DL, Roberts C, Parker GJ, Logue JP, Hutchinson CE. Prostate cancer: evaluation of vascular characteristics with dynamic contrast-enhanced T1-weighted MR imaging--initial experience. Radiology 2004;233:709–715.
13. Kiessling F, Lichy M, Grobholz R, et al. Simple models improve the discrimination of prostate cancers from the peripheral gland by T1-weighted dynamic MRI. Eur Radiol 2004;14:1793–1801.
14. Langer DL, van der Kwast TH, Evans AJ, et al. Prostate tissue composition and MR measurements: investigating the relationships between ADC, T2, K(trans), v(e), and corresponding histologic features. Radiology 2010;255:485–494.
15. Tekes A, Kamel I, Imam K, et al. Dynamic MRI of bladder cancer: evaluation of staging accuracy. AJR Am J Roentgenol 2005;184:121–127.
16. Nguyen HT, Pohar KS, Jia G, et al. Improving bladder cancer imaging using 3-T functional dynamic contrast-enhanced magnetic resonance imaging. Invest Radiol 2014;49:390–395.
17. Shi L, Wang D, Liu W, et al. Automatic detection of arterial input function in dynamic contrast enhanced MRI based on affinity propagation clustering. J Magn Reson Imaging 2014;39:1327–1337.
18. Workie DW, Dardzinski BJ, Graham TB, Laor T, Bommer WA, O'Brien KJ. Quantification of dynamic contrast-enhanced MR imaging of the knee in children with juvenile rheumatoid arthritis based on pharmacokinetic modeling. Magn Reson Imaging 2004;22:1201–1210.
19. Parker GJM, Roberts C, Macdonald A, et al. Experimentally-derived functional form for a population-averaged high-temporal-resolution arterial input function for dynamic contrast-enhanced MRI. Magn Reson Med 2006;56:993–1000.
20. Willinek WA, Gieseke J, Kukuk GM, et al. Dual-source parallel radiofrequency excitation body MR imaging compared with standard MR imaging at 3.0 T: initial clinical experience. Radiology 2010;256:966–975.

21. Shah ZK, Elias SN, Abaza R, et al. Performance comparison of 1.5-T endorectal coil MRI with 3.0-T nonendorectal coil MRI in patients with prostate cancer. Acad Radiol 2015;22:467–474.

22. Johnson LM, Turkbey B, Figg WD, Choyke PL. Multiparametric MRI in prostate cancer management. Nat Rev Clin Oncol 2014;11:346–353.

23. Pinaquy JB, De Clermont-Galleran H, Pasticier G, et al. Comparative effectiveness of [(18) F]-fluorocholine PET-CT and pelvic MRI with diffusion-weighted imaging for staging in patients with high-risk prostate cancer. Prostate 2015;75:323–331.

24. Kalavagunta C, Michaeli S, Metzger GJ. In vitro Gd-DTPA relaxometry studies in oxygenated venous human blood and aqueous solution at 3 and 7 T. Contrast Media Mol Imaging 2014;9:169–176.

25. Stollberger R, Wach P. Imaging of the active B-1 field in vivo. Magn Reson Med 1996;35:246–251.